Distribution Category:
Magnetic Fusion Energy Systems
(UC-423)

ANL/FPP/TM-265

ARGONNE NATIONAL LABORATORY
9700 South Cass Avenue
Argonne, Illinois 60439-4801

ANALYSIS OF THE NEUTRON GENERATION FROM A D-Li NEUTRON SOURCE

by

Itacil Gomes
Fusion Power Program
Technology Development

February 1994

Work supported by
Office of Fusion Energy
U.S. Department of Energy
under Contract W-31-109-Eng-38

TABLE OF CONTENTS

LIST OF FIGURES

LIST OF TABLES

ANALYSIS OF THE NEUTRON GENERATION FROM A D-Li NEUTRON SOURCE

I. Gomes

ABSTRACT

The study of the neutron generation from the D-Li reaction is an important issue to define the optimum combination of the intervening parameters during the design phase of a D-Li neutron source irradiation facility. The major players in defining the neutron yield from the D-Li reaction are the deuteron incident energy and the beam current, provided that the lithium target is thick enough to stop all incident deuterons. The incident deuteron energy also plays a role on the angular distribution of the generated neutrons, on the energy distribution of the generated neutrons, and on the maximum possible energy of the neutrons.

The D-Li reaction produces neutrons with energies ranging from eV's to several MeV's. The angular distribution of these neutrons is dependent on the energy of both, incident deuterons and generated neutrons. The deuterons lose energy interacting with the lithium target material in such a way that the energy of the deuterons inside the lithium target varies from the incident deuteron energy to essentially zero.

The first part of this study focuses in analyzing the neutron generation rate from the D-Li reaction as a function of the intervening parameters, in defining the source term, in terms of the energy and angular distributions of the generated neutrons, and finally in providing some insights of the impact of varying input parameters on the generation rate and correlated distributions. In the second part an analytical description of the Monte Carlo sampling procedure of the neutron from the D-Li reaction is provided with the aim at further Monte Carlo transport of the D-Li neutrons.

1. NEUTRON PRODUCTION FROM D-Li REACTION

The neutron production, from the interaction of highly energetic deuterons impinged in a lithium target, considering both the energy and the direction of the generated neutrons as a function of the deuteron energy was analyzed by F. Mann et. al. [1] and a triple differential cross section set was generated. This cross section set has the neutron yield as a function of discrete incident deuteron energy (1 MeV energy group width). For a given deuteron energy a double differential cross section is provided for discrete polar angles and energy groups of the generated neutrons. The azimuthal distribution of the generated neutrons is assumed uniform for each polar angle considered.

The neutron generation rate at an element of volume around a particular position "$\bar{r}$" inside the lithium target is calculated by taking the product of the macroscopic neutron yield cross section for the current deuteron energy by the number of deuterons at the element of volume considered. The energy and direction of the produced neutrons are defined by the double differential cross section which gives the probability of the neutrons been generated at each neutron energy group and angular bin. Thus, the source term at the position "$\bar{r}$" inside the lithium column as a function of the neutron energy and direction can be expressed by

$$S\left(\bar{r},E_n,\bar{\Omega}\right)=N\frac{d^2\sum\left(E_d,E_n,\bar{\Omega}\right)}{dE_n d\Omega}\delta\Omega\delta E_n\delta x \qquad (1)$$

where

$$N = I(y,z)\, N_O\, \partial y\, \partial z \qquad (2)$$

where "N_O" is the total number of deuterons incident in the Lithium target, I(y,z) is the deuteron current density distribution along the beam cross sectional area (what has an integral over the cross sectional area equal to unit), $d^2\Sigma(E_d,E_n,\Omega)/dE_n d\Omega$ is the D-Li reaction differential macroscopic cross section for generating neutrons with energy within the interval ∂E_n around E_n, and direction within the interval $\partial\Omega$ around Ω, and ∂x is the distance in the x-direction around "$\bar{r}$", which in this case is equal to the distance traveled inside the lithium target by a deuteron with energy E_d until it loses ∂E_d of its energy (equal to the width of the deuteron energy groups, which is equal to 1 MeV). It should be noticed that defining the deuteron energy E_d the position "x" along the beam direction is also defined. The value of the function I(y,z) is defined based on the deuteron density distribution along the cross sectional area of the beam when it hits the target.

When calculating "N" (number of deuterons at the position "$\bar{r}$") it is assumed that the absorption or loss of deuterons is neglectful, and as a consequence the number of deuterons is assumed constant throughout the lithium thickness. Also, it is assumed that the deuterons do not change direction due to interactions with the lithium atoms, and such as the function I(y,z) is constant throughout the lithium target thickness.

The number of deuterons incident on the lithium target is directly proportional to the deuteron beam current and obeys the following relationship

$$N = 6.242 \times 10^{18} \times \text{current}$$

where current is given in amperes, and N is given in deuterons per seconds (1 Ampere = 1 Coulomb/second = 6.242×10^{18} electron-charges/second). The evaluation of $d^2 \Sigma(E_d, E_n, \Omega)/ dE_n d\Omega$ is performed by multiplying the cross section from the D-Li reaction cross section data set for neutron production by the number density of the lithium target and by 10^{-3} (since the cross sections are given in milibarn per steradian (sr) per MeV).

The energy distribution of the neutrons at the generation point (independent to at which position the neutron was generated inside the lithium target) as a function of the incident deuteron energy is presented in Table 1. It can be noticed that most of the neutrons are generated with energies below 15 MeV (about 90%) and that the high energy component of the spectrum (above 20 MeV) is small and increases as the incident deuteron energy increases. The total number of neutrons generated as well as the average neutron energy at the source also increases as one increases the incident deuteron energy.

Figure 1 displays the neutron average energy at the generation point as a function of the incident deuteron energy. It can be noticed that the average neutron energy increases almost linearly with the incident deuteron energy. Figure 2 displays the variation of the neutron yield as a function of the deuteron energy. It can be noticed that going from 30 MeV-deuteron beam to a 40 MeV-deuteron beam the neutron yield increases by 60% what is almost twice the percentile of increase in the deuteron energy. Figure 3 presents the total neutron generation rate and above 20 MeV neutron generation rate as a function of the incident deuteron energy. As it can be noticed the component above 20 MeV grows faster with the incident deuteron energy than the total neutron generation rate.

Table 1
Comparison of Neutron Generation Rate, Average Energy, and Energy Distribution for Three Incident Deuteron Energies

	Deuteron Incident Energy		
	30 Mev	35 MeV	40 MeV
Percentage of Neutrons Born in Each Energy (MeV) Interval (%)			
from 0 to 15	91.94	88.12	84.33
from 15 to 21	5.51	7.63	9.28
from 21 to 32	2.12	3.54	5.39
from 32 to 43	0.42	0.66	0.90
from 43 to 50	0.0022	0.059	0.10
Total Neutron Generation rate for a 250 mA D-beam (neutrons/sec)	6.460e+16	8.364e+16	1.035e+17
Average Neutron Energy (MeV)	5.36	6.06	6.71

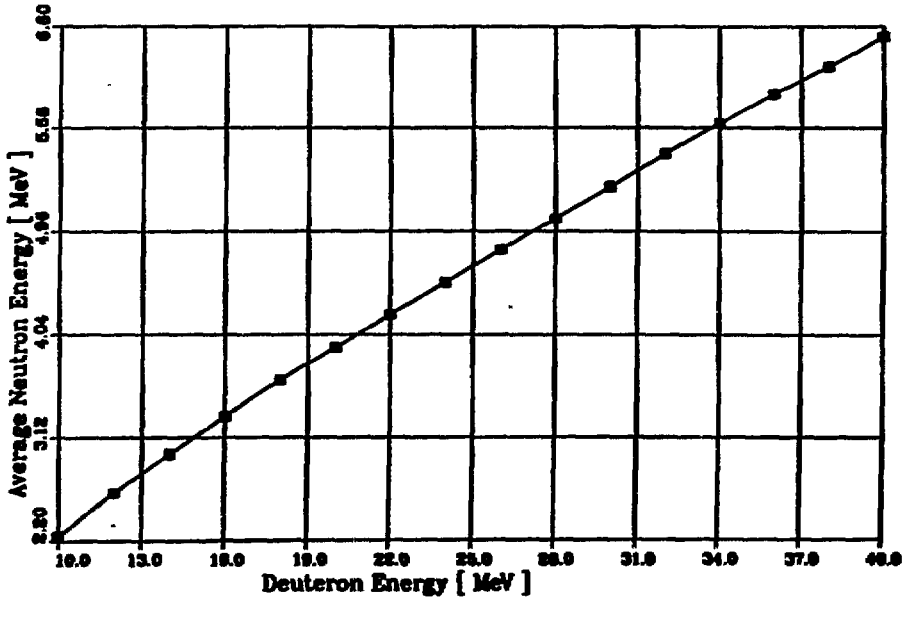

Figure 1. Average energy of the neutrons as a function of the deuteron incident energy.

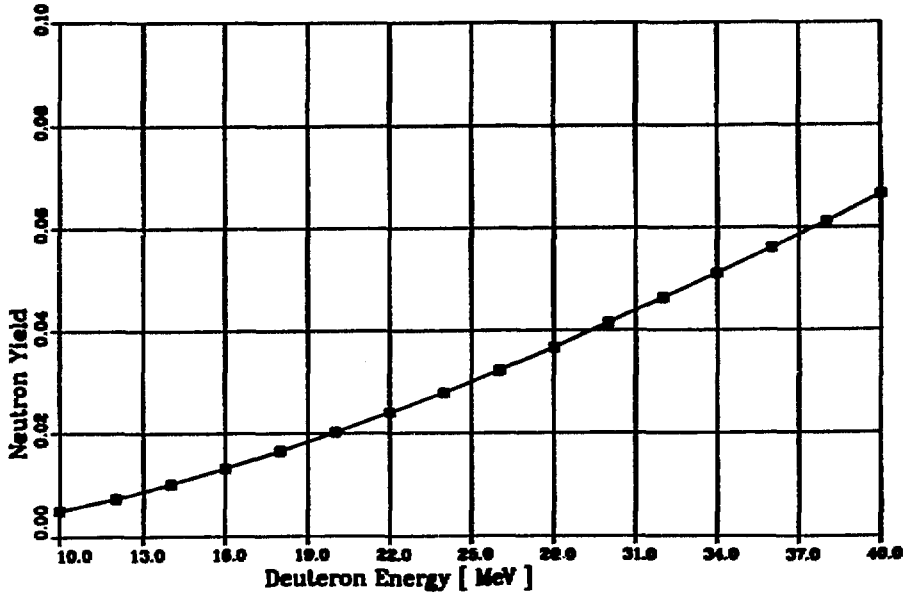

Figure 2. Neutron yield as a function of the incident deuteron energy.

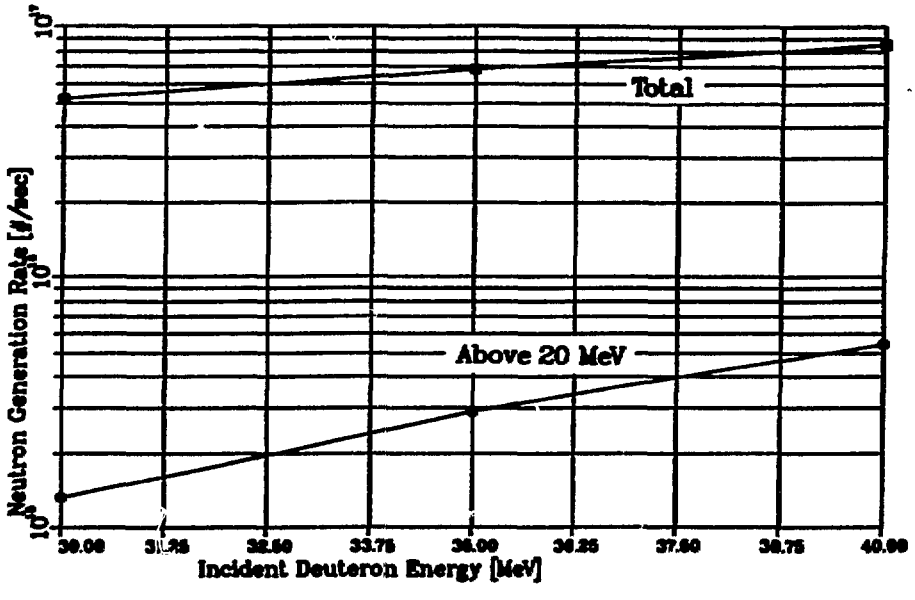

Figure 3. Generation rate of neutrons with energy above 20 MeV compared with the total neutron generation rate as a function of the incident deuteron energy.

Figures 4, 5, and 6 present the neutron generation rate per 1 MeV deuteron energy interval for a 250 mA deuteron beam as a function of the position inside the lithium target for three different incident deuteron energies, 10, 30, and 40 MeV, respectively. Each point presented in these plots represents the neutron production for a particular deuteron energy bin and its approximated location inside the lithium target. It can be noticed that for deuteron energies below 10 MeV the neutron generation decreases significantly (for a incident deuteron energy of 10 MeV the neutron yield is only 0.0053 or less than 10% of the neutron yield for a 35 MeV deuteron beam).

Figures 7, 8, and 9 present the neutron spectrum of the generated neutrons for 10, 30, and 40 MeV deuteron beams, respectively considering a 250 mA deuteron beam current. The values in these plots represent the neutron generation rate integrated over all angles, all possible deuteron energies (from zero to the incident deuteron energy) and within each particular neutron energy group (1 MeV width each neutron group).

Figure 10, 11, and 12 present the neutron generation rate as a function of polar angle of the generated neutrons for 10, 30, and 40 MeV incident deuteron energy. Each point presented in these plots represent the neutron generation rate integrated over the deuteron energies, neutron energy group, and within the polar angle bin considered (each polar angle has a 5° length, except the first and the last ones which have a 2.5° length). Each plot has 6 (six) curves, being one for the total generation rate over the neutron energies and other 5 (five) representing 5 neutron energy groups as it is indicated into the legend of the plot. It can be noticed from these plots that higher the neutron energy more forward peaked is the angular distribution of the generated neutrons, lower the energy more isotropic the distribution. Also, it is important to point out that the most forward and backward angles have the smallest weight during the integration, what translates in having the most forward direction (which has the highest cross section per steradian) with less neutrons than other directions.

2. NEUTRON SOURCE TERM FOR PARTICLE TRANSPORT

To perform the transport of the neutrons generated from the D-Li reaction using a Monte Carlo code [2,3] it is necessary to sample the phase space coordinates of the generated particle from probability distributions based on the deuterium-lithium interaction cross sections. This section describes the neutron source term sampling process.

The following steps were adopted to define probability distribution tables and to perform the sampling process for neutrons' starting spatial coordinates, energy, and direction:

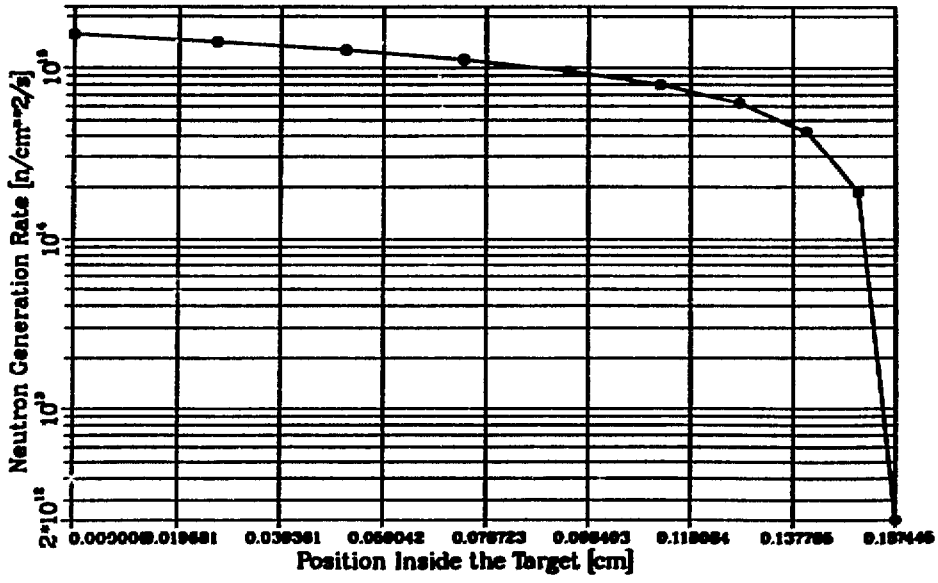

Figure 4. Neutron generation rate per 1 MeV deuteron energy loss as a function of the position inside the lithium target for a 10 MeV incident deuteron energy.

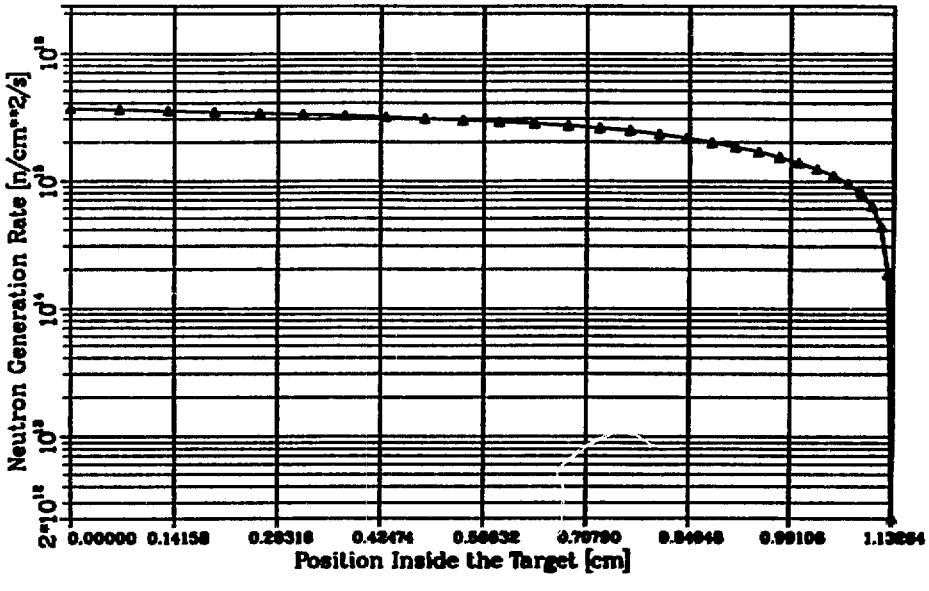

Figure 5. Neutron generation rate per 1 MeV deuteron energy loss as a function of the position inside the lithium target for a 30 MeV incident deuteron energy.

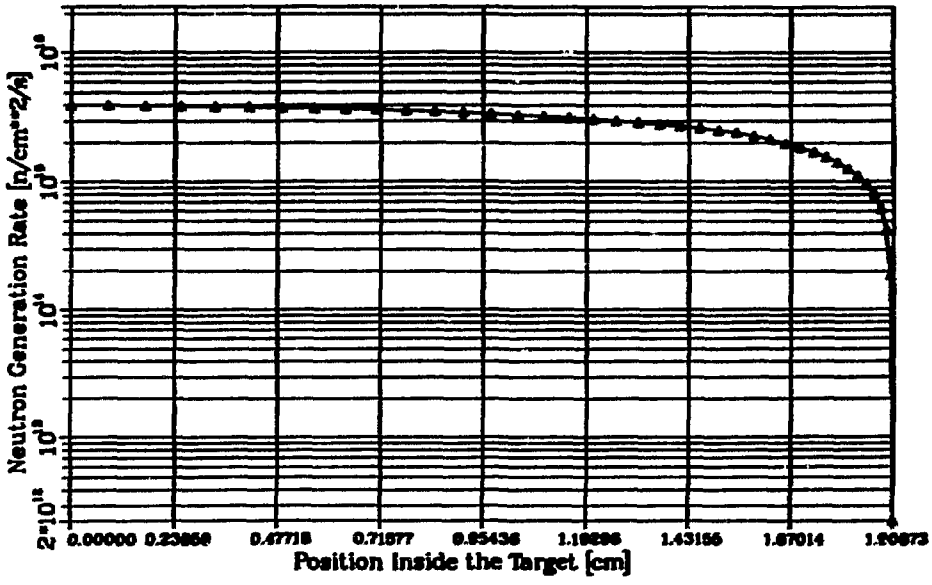

Figure 6. Neutron generation rate per 1 MeV deuteron energy loss as a function of the position inside the lithium target for a 40 MeV incident deuteron energy.

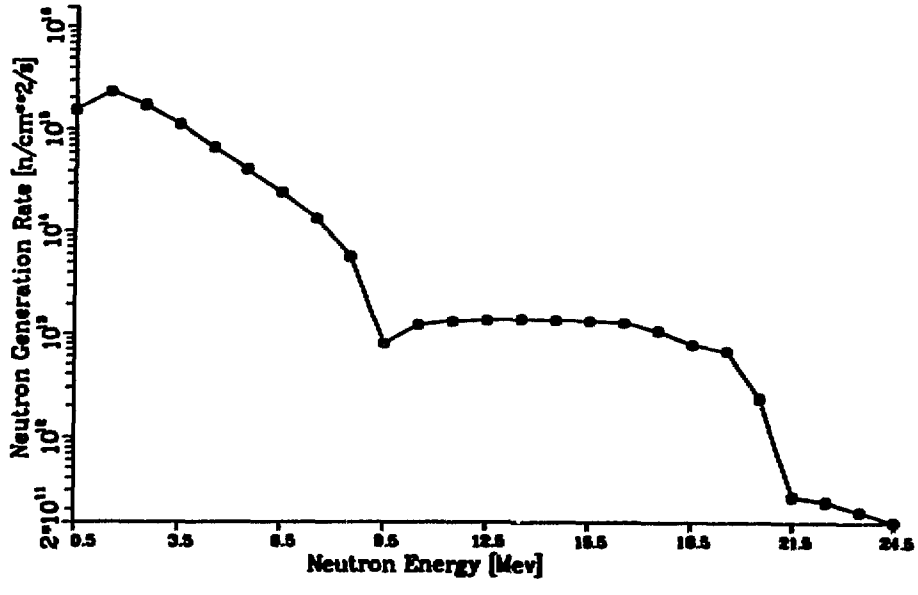

Figure 7. Neutron energy spectrum per MeV at the generation points for a incident deuteron beam energy of 10 MeV.

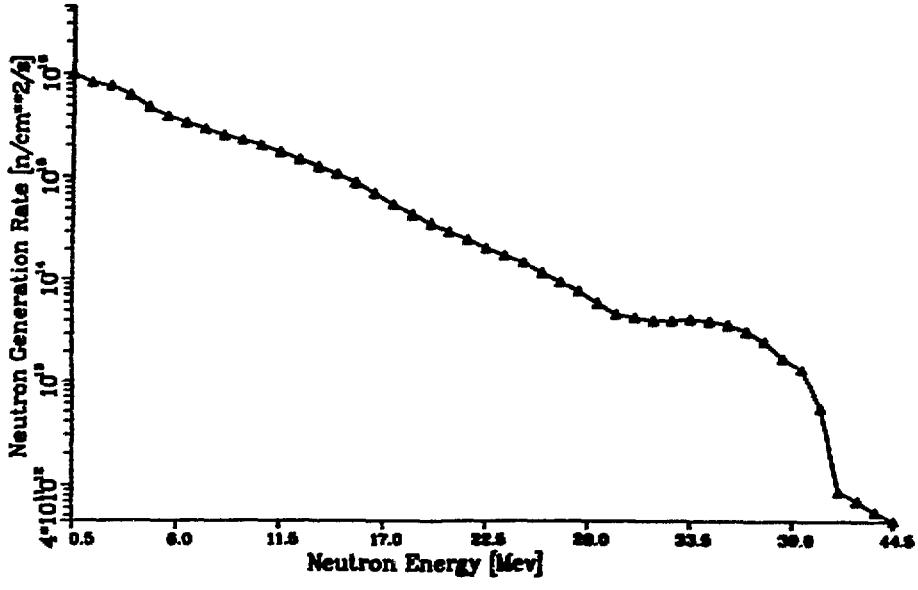

Figure 8. Neutron energy spectrum per MeV at the generation points for a incident deuteron beam energy of 30 MeV.

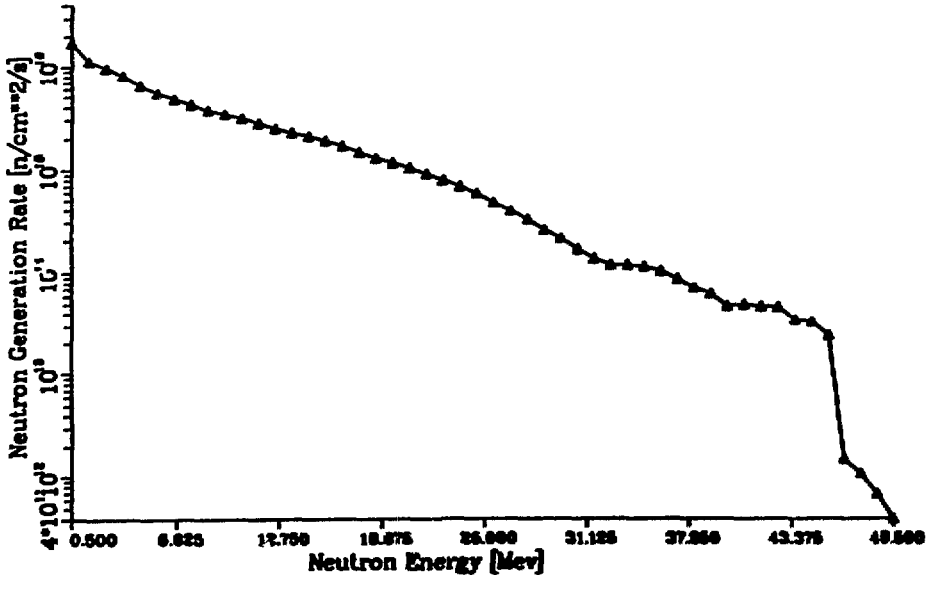

Figure 9. Neutron energy spectrum per MeV at the generation points for a incident deuteron beam energy of 40 MeV.

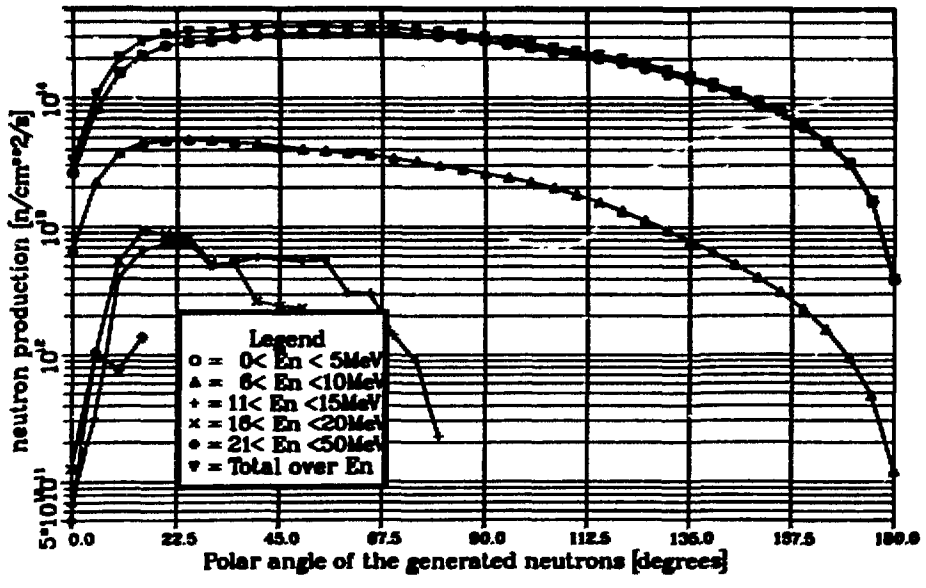

Figure 10. Neutron generation rate as a function of the polar angle of the generated neutrons for an incident deuteron energy of 10 MeV.

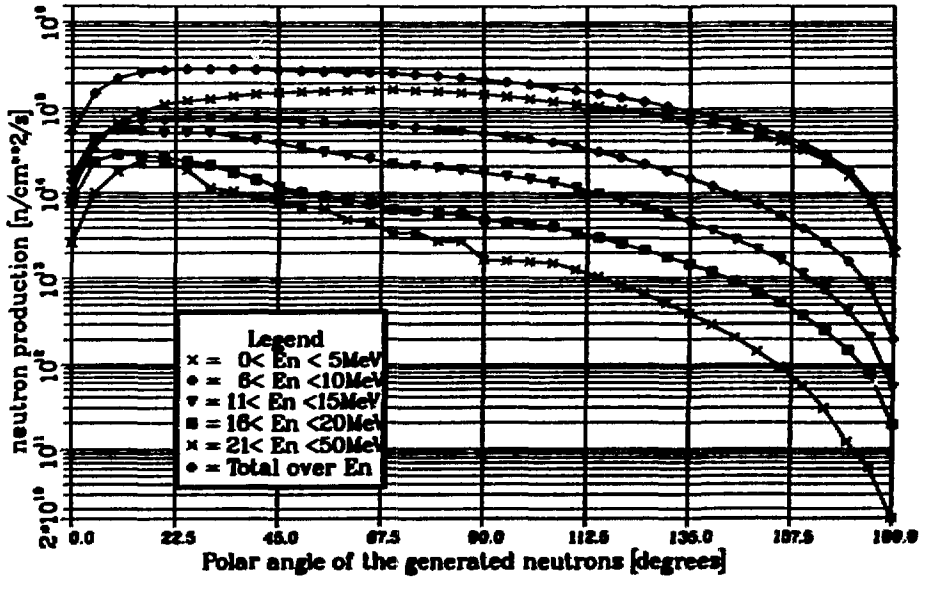

Figure 11. Neutron generation rate as a function of the polar angle of the generated neutrons for an incident deuteron energy of 30 MeV.

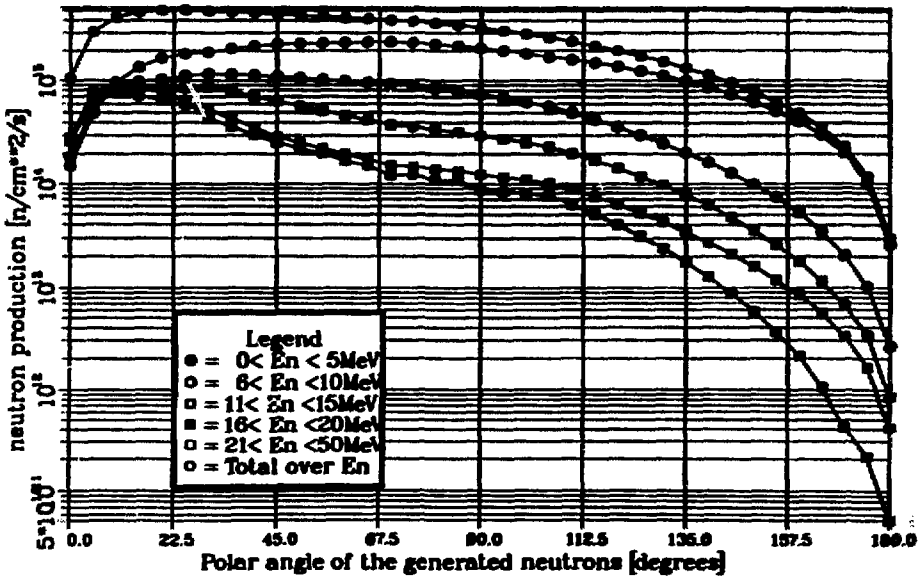

Figure 12. Neutron generation rate as a function of the polar angle of the generated neutrons for an incident deuteron energy of 40 MeV.

1. The first step is to select a position at which the reaction D-Li is going to occur or in other words the deuteron energy for the reaction. Here two components are the major players, the first is the lithium "stopping power" for deuterons, and the second the D-Li reaction cross section for each possible deuteron energy into the system.

The stopping power formulation used in this work was the following:

$$\frac{dE}{dx} = \frac{4\pi e^4 z^2}{m_o V^2} NZ\left[\ell n \frac{2m_o V^2}{I} - \ell n\left(1-\beta^2\right) - \beta^2\right] \qquad (3)$$

where dE is the energy decrement (as excitation and ionization) of a deuteron with energy E_d as it travels a distance "dx" inside the lithium target material. "I" is the mean atomic excitation potential, "m_o" is the rest mass of an electron, "e" the electron charge, "z" is the atomic number of the deuteron, "Z" is the atomic number of the Lithium target, "N" the number density of the lithium target (atoms/cm^3), and "V" is the deuteron velocity (=ßc).

Since the cross section data set for the D-Li reaction has discrete deuteron energies from 1 to 40 MeV with intervals of 1 MeV each, 1 MeV is the energy loss for the Deuteron that one is interested. If one plugs into the stopping power formulation 1 MeV (performing the necessary integration) as the decrement of the deuteron energy ("dE") it is possible to define the distance traveled by the deuteron within each deuteron energy bin of the cross section table.

Now, if one multiplies the distance traveled by the deuteron within each energy interval (from the incident energy to zero) by the corresponding D-Li cross section value for neutron generation of that deuteron energy interval, it is possible to define the probability of the deuteron having an interaction (D-Li reaction) per energy interval. Based on that it is possible to sample the deuteron energy for the interaction from:

$$\frac{\sum_{i=1}^{m}\Delta x_i \Sigma(E_i)}{\Sigma_t} \le R \le \frac{\sum_{i=1}^{m+1}\Delta x_i \Sigma(E_i)}{\Sigma_t} \tag{4}$$

with

$$\Sigma_t = \sum_{i=1}^{M}\Sigma(E_i)\Delta x_i \tag{5}$$

where "M" is the total number of deuteron energy groups being analyzed, "i" is the index for deuteron energy group, "$\Sigma(E_i)$" is the total neutron production cross section from the D-Li reaction for the "i-th" deuteron energy group, and "R" is a random number. As soon as this relationship is satisfied the value of "m" defines the selected deuteron energy group at which the D-Li reaction is going to occur.

The range of the deuterons inside the lithium target can be defined as:

$$R_g = \sum_{i=1}^{M}\Delta x_i \tag{6}$$

Based on Eq. (4) it is possible to define the segment on the x-axis inside the lithium target of the D-Li interaction. To define the x-coordinate value it is assumed an uniform distribution for the points inside the selected segment, and the following selection is performed:

$$R = \frac{\int_{x_o}^{x} dx}{\int_{x_o}^{x_1} dx} \tag{7}$$

where, "R" is a random number, "x_0" is the lower limit of the selected interval, "x_1" is the upper limit, and "x" the sampled point inside the interval.

The other remaining spatial coordinates (y and z) for the point where the reaction occurs are sampled from uniform distributions within the limits of the beam spot area on the lithium target. Please note that here it is considered uniform deuteron density distribution along the beam cross sectional area, otherwise one should sample from the actual density distribution for the deuteron beam.

2. To select the neutron polar angle bin the following sampling scheme is adopted:

$$\frac{\sum_{i=1}^{k} W(\theta_i)\Sigma(E_m,\theta_i)}{\Sigma_t(E_m)} \le R \le \frac{\sum_{i=1}^{k+1} W(\theta_i)\Sigma(E_m,\theta_i)}{\Sigma_t(E_m)} \tag{8}$$

with

$$\Sigma_t(E_m) = \sum_{i=1}^{K} \Sigma(E_m, \theta_i)\, W(\theta_i) \tag{9}$$

where, "R" is a random number, "E_m" is the previously selected deuteron energy, $W(\theta_i)$ is the weight of the polar angle interval "θ_i" on the 4π sphere, and "$\Sigma(E_m,\theta_i)$" is the D-Li reaction cross section for the deuteron energy E_n, and polar angle interval θ_i.

The polar angle is sampled from an uniform distribution within the selected interval "k". The azimuthal angle is also sampled from an uniform distribution along the 2π span.

3. The neutron energy group is sampled based on the probability distribution constructed from the cross section values for the 50 (fifty) possible neutron energy groups (1 MeV interval each) for the already selected deuteron energy group and polar angle bin. Again, a simple sampling scheme is adopted, as follows:

$$\frac{\sum_{i=1}^{j}\Sigma(E_m,\theta_k,E_i)}{\Sigma_t(E_m,\theta_k)} \le R \le \frac{\sum_{i=1}^{j+1}\Sigma(E_m,\theta_k,E_i)}{\Sigma_t(E_m,\theta_k)} \tag{10}$$

where:

$$\Sigma(E_m,\theta_k) = \sum_{i=1}^{J}\Sigma(E_m,\theta_k,E_i) \tag{11}$$

The actual neutron energy is sampled from an uniform distribution inside the selected energy interval "j". It should be noted that, this is an approximation and it is accurate enough for energies above 1 or 2 MeV, where the neutron interaction cross section is, in most cases, not highly energy dependent within an 1 (one) MeV energy interval. For neutron energies below 1 MeV (or for the neutron energy interval between 0 and 1 MeV) this approximation may not be acceptable since there are several neutron reactions (example: tritium and helium generation in lithium, boron, etc.) which are highly energy dependent. Then, when computing these responses a better description of the neutron generation in this interval would be required.

3. CONCLUSIONS

The incident deuteron energy can have an important impact on the neutron generation rate from the D-Li reaction, suggesting that the trade-offs between higher beam current or higher incident deuteron energy should be explored in deep. The presence of very high energy neutrons, when high energy deuterons are used, should not be of great concern, since the percentiles at which they are present are very small. No advantage could be envisaged, during this work, in lowering the deuteron energy, and as a consequence it is recommended the use of the highest deuteron energy which still produces acceptable levels of nuclear responses and correspondent ratio between them for fusion material testing applications.

REFERENCES

1. Mann, F.M., Schmittroth, F., and Carter, L.L., "Neutrons from D+Li and the FMIT Irradiation Environment," Hanford Engineering Development Laboratory Report HEDL-TC-1459 (1981).

2. Briesmeister, J., Editor, "MCNP - A General Monte Carlo Code for Neutron and Photon Transport," LA-7396-M (9186).

3. Emmett, M.B., Editor, "MORSE-CGA - A Monte Carlo Radiation Transport Code with Array Geometry Capability," Oak Ridge National Laboratory Report ORNL-6174 (1985).

DISTRIBUTION LIST FOR ANL/FPP/TM-265

Internal

H. Attaya
S. Bhattacharyya
M. Billone
J. Brooks
H. Chung
D. Ehst
I. Gomes (5)
D. Gruen
A. Hassanein
H. Herman
T. Hua
C. Johnson
T. Kassner
A. Krauss
M. Lineberry
B. Loomis
S. Majumdar
R. Mattas
K. Natesan
J.-H. Park
B. Picologlou
C. Reed
D.L. Smith
D.-K. Sze
L. Turner
FPP Files (10)
TIS Files

External

DOE/OSTI for distribution per UC-423 (48)
Manager, Chicago Operations Office
ANL-E Libraries (2)
ANL-W Library
M. Abdou, University of California, Los Angeles
J. Anderson, Los Alamos National Laboratory
C. Baker, Oak Ridge National Laboratory
J. Bartlit, Los Alamos National Laboratory
S. Berk, U.S. Department of Energy
T. Burchell, Oak Ridge National Laboratory
R. Causey, Sandia National Laboratories, Livermore
M. Cohen, U.S. Department of Energy
C. Croessman, Sandia National Laboratories, Albuquerque
W. Daenner, ITER, Germany
J. Davis, McDonnell Douglas Astronautics Company
H. Dodds, University of Tennessee
J. Doggett, Lawrence Livermore National Laboratory
D. Doran, Washington State University
L. El-Guebaly, University of Wisconsin
E. Embrechts, Rensselaer Polytechnic Institute
D. Gelles, Pacific Northwest Laboratories
N. Ghoneim, University of California, Los Angeles
Y. Gohar, ITER JCT, Garching, Germany
L. Greenwood, Pacific Northwest Laboratory
G. Kulcinski, University of Wisconsin
D. Lousteau, Fusion Engineering Design Center
F. Mann, Pacific Northwest Laboratories
D. Muntz, Kernforschungszentrum Karlsruhe, Germany
R. Nygren, Sandia National Laboratories, Albuquerque
A. Opdenaker, U.S. Department of Energy
S. Piet, ITER JCT, San Diego, California
D. Post, ITER JCT, San Diego, California
R. Price, U.S. Department of Energy
A. Raffray, ITER JCT, Garching, Germany
M. Sawan, University of Wisconsin
K. Schultz, General Atomic
M. Seki, Japan Atomic Energy Research Institute, Japan

T. Shannon, Fusion Engineering Design Center
D. Steiner, Rensselaer Polytechnic Institute
P. Stevens, University of Tennessee
I. Sviatoslavsky, University of Wisconsin
M. Tillack, University of Los Angeles, California
J. Vetter, Kernforschungszentrum Karlsruhe, Germany
G. Vieider, ITER, Germany
R. Watson, Sandia National Laboratories, Albuquerque
F.W. Wiffen, U.S. Department of Energy
L. Wittenberg, University of Wisconsin
K. Wilson, Sandia National Laboratories, Livermore
M. Youssef, University of California, Los Angeles
Bibliothek, Max-Planck-Institute fur Plasmaphysik, Germany
C.E.A. Library, Fontenay-aux-Roses, France
Librarian, Culham Laboratory, England
Thermonuclear Library, Japan Atomic Energy Research Institute, Japan